

## Supporting Information for

# Cu-nanoclusters supported on nanocrystalline SiO<sub>2</sub>-MnO<sub>2</sub>: a bifunctional catalyst for one step conversion of glycerol to acrylic acid

Bipul Sarkar,<sup>a</sup> Chandrashekar Pendem,<sup>a</sup> L. N. Sivakumar Konathala,<sup>a</sup> Ritesh Tiwari,<sup>a</sup> Takehiko Sasaki,<sup>b</sup> and Rajaram Bal\*<sup>a</sup>

### Materials

Copper (II) nitrate trihydrate (Cu(NO<sub>3</sub>)<sub>2</sub>·3H<sub>2</sub>O), Manganese(II) chloride (MnCl<sub>2</sub>), Tetraethyl orthosilicate (TEOS), Commercial MnO<sub>2</sub>, Cu<sub>2</sub>O and CuO were purchased from Sigma-Aldrich. Ethanol, Acetonitrile, cetyltrimethylammonium bromide (CTAB) were purchased from Merck KGaA, Darmstadt, Germany. All the chemicals were used without further purification. Double distilled water was prepared with a BOROSIL® water distillation unit.

### Catalyst preparation

In a typical preparation method, a solution of Cu(NO<sub>3</sub>)<sub>2</sub>·3H<sub>2</sub>O (0.0749 g) was added drop wise into a solution of MnCl<sub>2</sub>·2H<sub>2</sub>O (15.34 g) containing 2.6 g TEOS under vigorous stirring. Subsequently, a solution of cetyltrimethylammonium bromide (CTAB) was added to the reaction mixture of two metal precursors (Cu : CTAB : H<sub>2</sub>O = 1 : 0.7 : 250 molar ratio). After stirring, until a homogeneous solution was obtained, the resultant mixed species was hydrothermally treated at 150°C for 24 h in a Teflon-lined autoclave vessel under an autogeneous pressure. The product was washed with distilled water and ethanol, and dried at ambient temperature for 10 h and at 100°C for 6 h. Finally the material was calcined at 500°C for 6 h in air. The prepared sample was denoted as (Wt% Cu)Cu/SiO<sub>2</sub>-MnO<sub>2</sub>. Conventional Cu catalysts over MnO<sub>2</sub> and SiO<sub>2</sub> were also prepared as reference using commercial MnO<sub>2</sub> and SiO<sub>2</sub> by incipient wetness impregnation method and denoted as (wt% Cu)Cu/MnO<sub>2</sub><sup>comm.</sup> & (wt% Cu)Cu/SiO<sub>2</sub><sup>comm.</sup>.

### Catalyst characterization

Powder x-ray diffraction (XRD) measurements were performed with a Bruker D8 advance x-ray diffractometer with a Cu K $\alpha$  radiation (40 kV and 30 mA) in the 2 $\theta$  range 5-60°. The SEM images are taken on a FEI Quanta 200 F, using ETD detector with an acceleration tension of 10 or 30 kV. All the Samples were analysed by spreading them on a carbon tape and coated with gold to increase the electrical conductivity. Energy dispersive X-ray spectroscopy (EDX) was used in connection with SEM for the elemental analysis. The elemental mapping was also performed with the same spectrophotometer. The morphology, lattice fringes and crystal boundaries of the samples were examined using a JEOL JEM 2100 high-resolution transmission electron microscope (HRTEM). Samples are mounted by dispersing on ethanol on a lacey carbon Formvar coated Cu grid. X-Ray photoelectron spectra (XPS) of the catalysts were recorded with a Thermo Scientific K-Alpha X-Ray photoelectron equipped with Mg K $\alpha$  radiation. The C 1s peak at 284.8 eV was used as a calibration peak. Extended X-ray absorption fine structure spectroscopy (XAFS) measurements of Cu-K edge were carried out at the High Energy Accelerator Research Organization (KEK-IMMS-PF), Tsukuba, Japan. The EXAFS spectrum of the fresh catalyst was measured in the transition mode, whereas for the spent catalyst the EXAFS spectrum was measured in the fluorescence mode using a Lytle detector with Ar gas and spectra were taken at BL-7C and BL-9C at the Photon Factory, Tsukuba, Japan. The electron storage ring was operated at 2.5 GeV and 450 mA; synchrotron radiation from the storage ring was monochromatized by a Si(111) channel cut crystal. Ionized chamber, which were used as detectors for incident X-ray (I<sub>0</sub>) and transmitted X-ray (I), were filled with N<sub>2</sub> mixture gas, respectively. The angle of the monochromators was calibrated with Cu foil. The EXAFS raw data was analysed with UWXAFS analysis package<sup>1</sup> including background subtraction program AUTOBK<sup>2</sup> and curve fitting program FEFFIT.<sup>3</sup> The amplitude reducing factor, S<sub>0</sub><sup>2</sup> was fixed at

1.0. The backscattering amplitude and phase shift were calculated theoretically by FEFF 8.4 code.<sup>4</sup> ATOMS<sup>5</sup> were used to obtain FEFF input code for crystalline materials. Temperature programmed reduction (TPR) experiment were carried out in a Micromeritics, Auto Chem II 2920 instrument connected with a thermal conductivity detector (TCD). Prior to TPR, the catalysts were also heated at 650°C for 2 h in helium and then placed in 10% H<sub>2</sub>/Ar with a flow rate of 40 mL min<sup>-1</sup> in the temperature range of 40-1000 °C with an increment of 10 °C/min. The amount and strength of the acid site were analysed by ammonia Temperature programmed desorption (TPD) technique using the same Micromeritics, Auto Chem II 2920 instrument. About 0.1 g sample was saturated with NH<sub>3</sub> at 100°C and flashed with He to remove the physically adsorbed NH<sub>3</sub>, finally the decomposition of NH<sub>3</sub> was carried at a heating rate of 10°C/ min under He flow.

### Glycerol oxydehydration

Glycerol oxydehydration was carried out in liquid phase using a 50 ml double necked round bottom flask containing 0.01 mol (0.92 g) glycerol and 0.046 g of Cu/SiO<sub>2</sub>-MnO<sub>2</sub> catalyst in 10 ml solvent (acetonitrile). The reaction mixture was kept at 70°C and H<sub>2</sub>O<sub>2</sub> (50 wt. % in H<sub>2</sub>O) was added in 0.5 ml portion with a time interval of 15 min. The reaction products were identified by GC-MS (HP 5890 GC coupled with 5972 MSD). The identified product was analysed in an Agilent 7890, fitted with a MXT-WAX (30m X 0.28mm i.d., 0.25 µm film thickness) capillary column and a FID detector. The activity of the catalyst was calculated as:

$$\text{Conversion (C\%)} = \frac{\text{Moles of glycerol reacted (C\%)}}{\text{Moles of glycerol initially used (C\%)}} \times 100$$

$$\text{Selectivity (C\%)} = \frac{\text{Moles of product (C\%)}}{\text{Moles of glycerol reacted (C\%)}} \times 100$$

The presence of peroxo intermediate at the end of the reaction was checked using phosphine at the end of the reaction. The product was identified by GC-MS as well as TLC (thin layer chromatography).

1. E. A. Stern, M. Newvill, B. Ravel, Y. Yacoby and D. Haskel, *Phys. B*, 1995, **117**, 208.
2. M. Newvill, P. Livins, Y. Yacoby, E. A. Stern and J. Rehr, *J. Phys. Rev. B: Condens. Matter*, 1993, **47**, 14126.
3. A. L. Aukudinov, B. Ravel, J. J. Rehr and S. D. Conradson, *Phys. Rev. B: Condens. Matter*, 1998, **58**, 7565.
4. A. L. Ankudinov, A. I. Nesvizhskii and J. Rehr, *J. Phys. Rev. B: Condens. Matter*, 2003, **67**, 115120.
5. R. Ravel, *J. Synchrotron Radiat.*, 2001, **8**, 314.

Figure S1

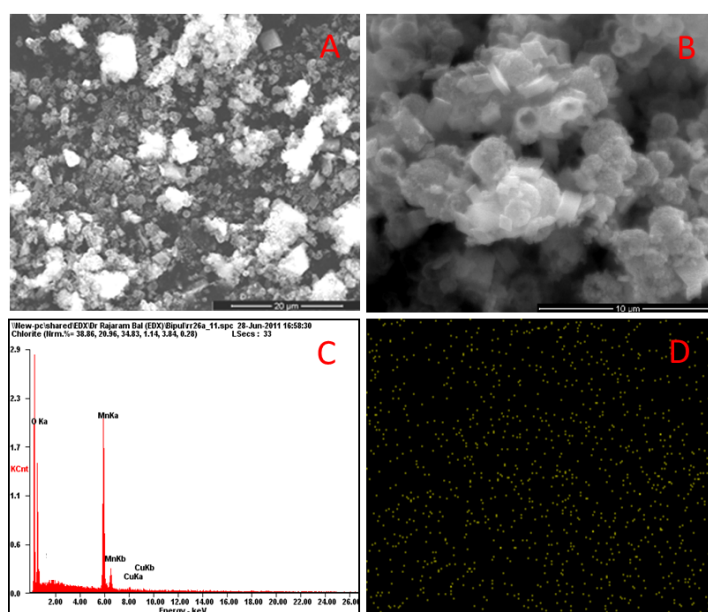


Figure S1 SEM micrograms of Cu/SiO<sub>2</sub>-MnO<sub>2</sub> catalyst synthesized by (A) impregnation method and (B) hydrothermal method; (C) & (D) are the EDAX and elemental mapping of Cu of the hydrothermally prepared catalyst, respectively.

Figure S2

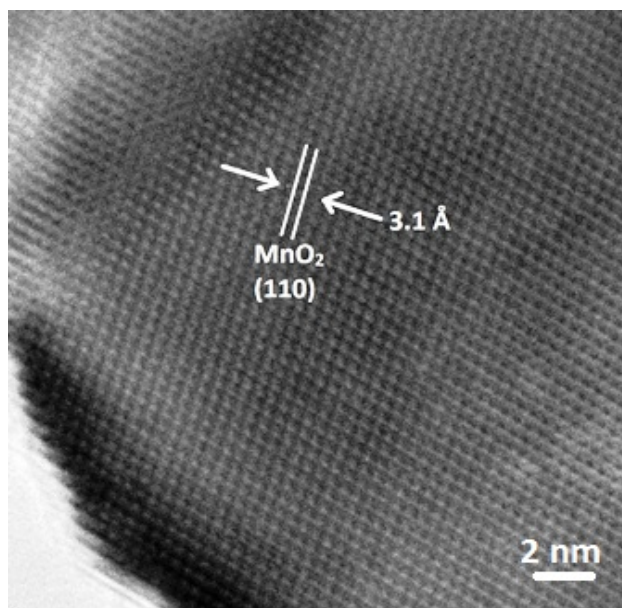


Figure S2. HRTEM image of hexagonal MnO<sub>2</sub> showing lattice fringes with a d-spacing of 110 plane of hexagonal MnO<sub>2</sub>.

Figure S3

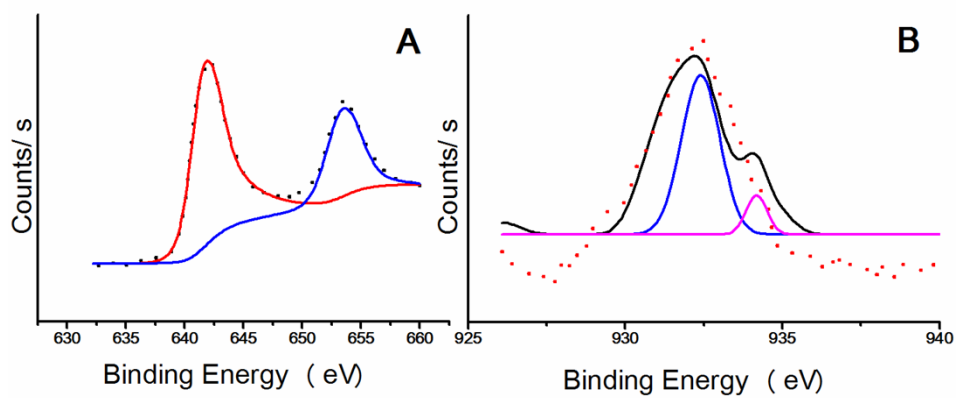


Figure S3. Photoelectron spectra of A) Mn 2p & B) Cu 2p prepared by hydrothermal method (0.9%Cu/SiO<sub>2</sub>-MnO<sub>2</sub>, fresh catalyst)

Figure S4

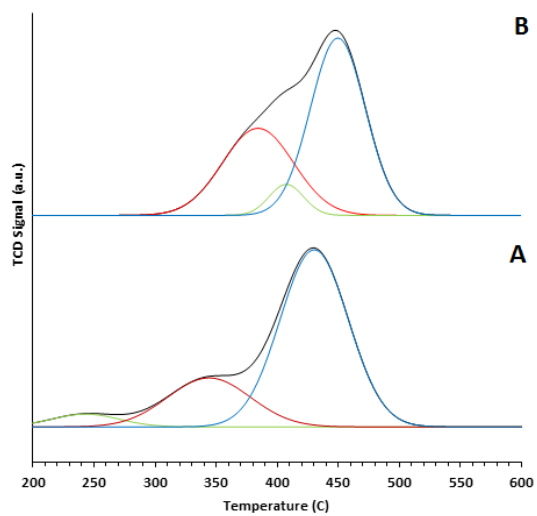


Figure S4. TPR profile of A) 0.9%Cu/SiO<sub>2</sub>-MnO<sub>2</sub> and B) 1%Cu/SiO<sub>2</sub>-MnO<sub>2</sub><sup>imp</sup>

Figure S5

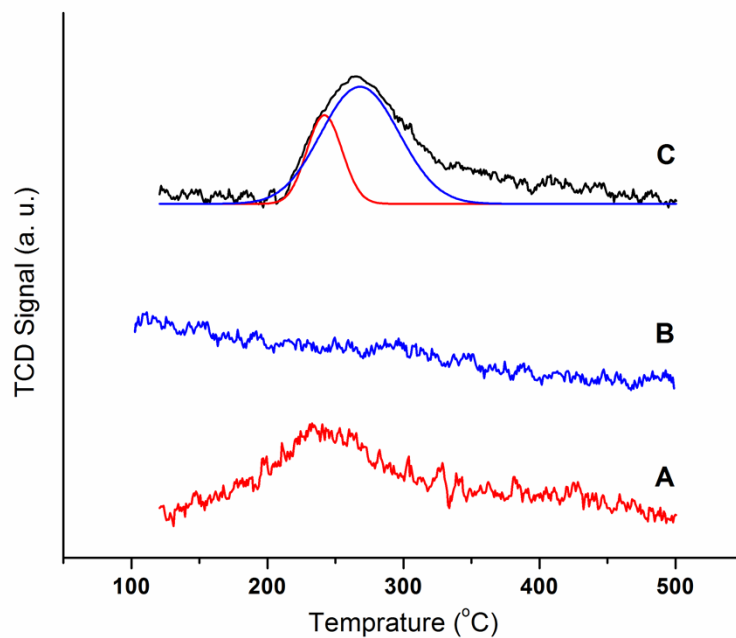


Figure S5. TPD-NH<sub>3</sub> patterns of hydrothermally prepared (A) SiO<sub>2</sub>; (B) commercial MnO<sub>2</sub> and (C) Cu/SiO<sub>2</sub>-MnO catalysts.

Figure S6

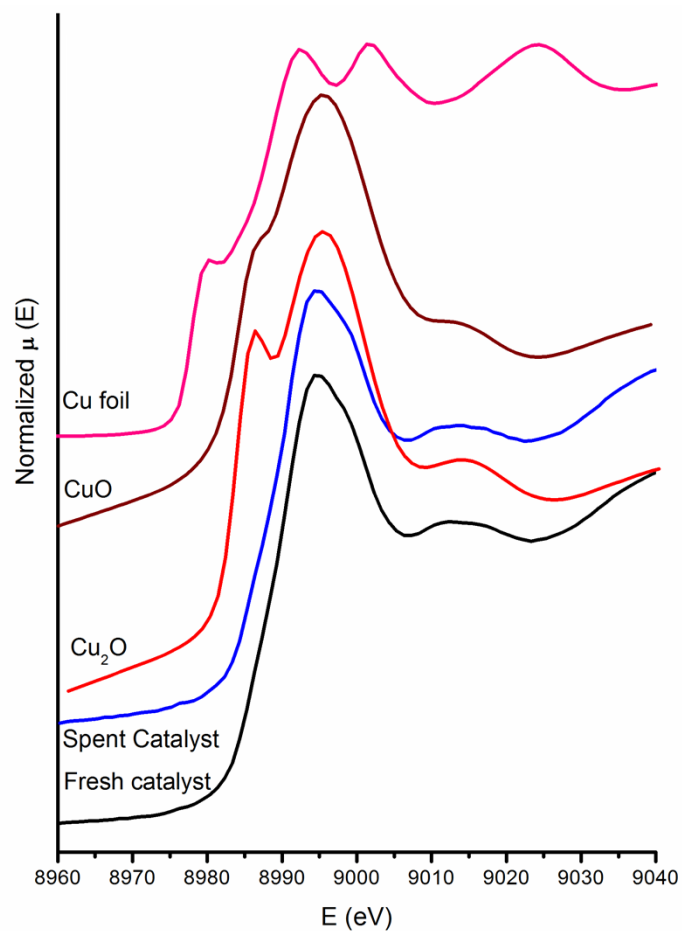


Figure S6. XANES spectra of Cu foil, commercial cuprous oxide, cupric oxide, fresh and spent 0.9%Cu/SiO<sub>2</sub>-MnO<sub>2</sub> catalyst.

Figure S7

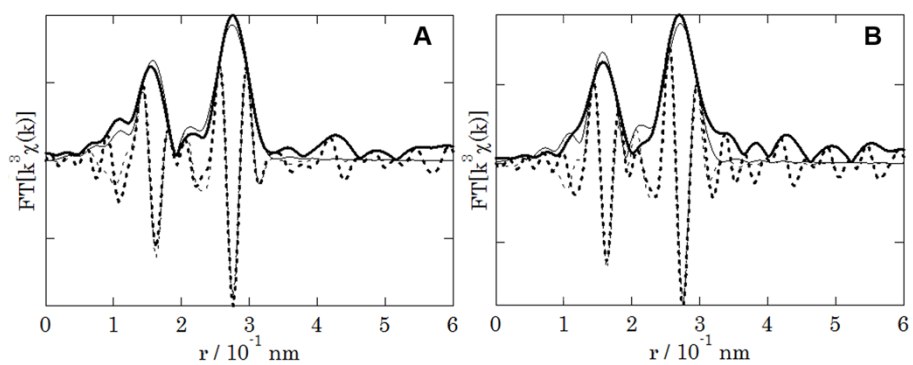


Figure S7. k<sub>3</sub>-weighted Fourier transform of Cu-K edge EXAFS for the A) fresh catalyst (0.9%Cu/SiO<sub>2</sub>-MnO<sub>2</sub>) and B) spent catalyst. Amplitude: solid curves; imaginary part: dotted curves; observed data: thick curves; fitting data: thin curves

Figure S8

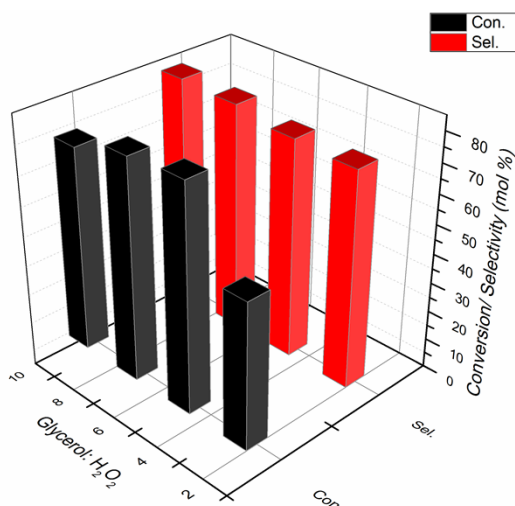


Figure S8. Influence of glycerol to H<sub>2</sub>O<sub>2</sub> ratio on oxydehydration of glycerol with 0.046g catalysts, 0.92g glycerol in 10 mL solvent were stirred at 70°C

Table S1. Summary of the EXAFS fitting results for Cu catalysts.

	Cu-O			Path	Cu <sub>2</sub> O crystal			$\Delta k$ (10nm <sup>-1</sup> )	$\Delta R$ (10 <sup>-1</sup> nm)	$\Delta E_0$ (eV)	$R_f$ (%)	
	R (10 <sup>-1</sup> nm)	CN	DW (10 <sup>-5</sup> nm <sup>2</sup> )		R (10 <sup>-1</sup> nm)	CN	DW (10 <sup>-5</sup> nm <sup>2</sup> )					Debye temp (K)
<b>Fresh</b>	1.954± 0.152	1.9±0.7	1.3±1.8	Cu-O	1.906±0. 064	4	27.2	286.0± 6.0	3 – 12	1.2 – 3.2	-5.3±1.5	2.22
				Cu-O-O	2.988	4	37.7					
				Cu-Cu	3.094	12	13.4					
<b>Spent (after 30h)</b>	1.951± 0.113	1.7±0.6	0.4±2.2	Cu-O	1.895±0. 013	4	27.1	286.6± 8.5	3 – 12	1.2 – 3.2	-7.4±2.1	4.02
				Cu-O-O	2.989	4	37.7					
				Cu-Cu	3.095	12	13.4					

Fitting was achieved with respect to Cu-O path and three paths of Cu<sub>2</sub>O crystal, which are repaired by ATOMS program and Cu<sub>2</sub>O crystal structure. Three paths of Cu<sub>2</sub>O crystal correspond to Cu-O(-Cu), multiple scattering of Cu-O-O(-Cu), and Cu-Cu(-Cu). These four paths are necessary for the good fitting. The simple two paths such as Cu-O and Cu-Cu, or the sole use of Cu<sub>2</sub>O crystal paths, or the CuO crystal structure failed. The former Cu-O path can be fitted as 0.1951 – 0.1954 nm that can be attributed to the distance of Cu<sup>2+</sup>-O of the monatomically dispersed Cu<sup>2+</sup> species. The crystal size of Cu<sub>2</sub>O is considered as small, since the inclusion of more distant paths does not improve the fittings.

Figure S9

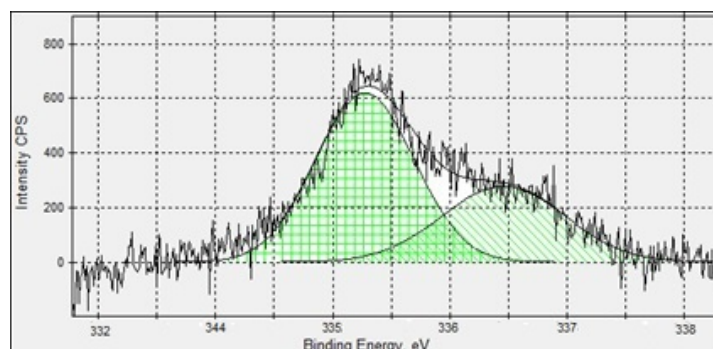


Figure S9. Cu LMM spectra of spent catalyst (after 3 h).

The Cu(LMM) Auger of the catalyst shows binding energies (eV) at 335.3 eV and 336.6 eV, which confirms the presence of Cu(+1) and Cu(+2) in the catalyst surface (without forming any metallic Cu).

Table S2. ICP-AES data of the reused catalyst for the oxydehydration of glycerol.

SI No	Run	Amount of Cu (wt%)
1	1 <sup>st</sup>	0.912
2	2 <sup>nd</sup>	0.910
3	3 <sup>rd</sup>	0.911
4	4 <sup>th</sup>	0.912

Table S3. Surface composition of 0.9%Cu/SiO<sub>2</sub>-MnO<sub>2</sub> catalyst as calculated from XPS.

SI No	Catalyst	Amount of Cu (At %)		
		Cu <sup>1+</sup>	Cu <sup>2+</sup>	
1	Fresh	0.9%Cu/SiO <sub>2</sub> -MnO <sub>2</sub>	90.12	9.88
2	Spent	0.9%Cu/SiO <sub>2</sub> -MnO <sub>2</sub>	89.23	11.77

Atomic ration of the Cu species was calculated taking all Cu species present in the catalyst as 100%.

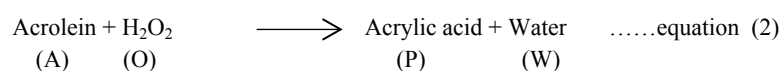
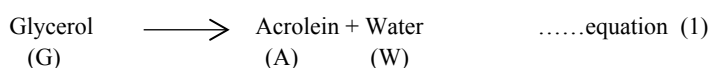
## Discussion

Glycerol consumption follow zero order reaction upto 5h and reaches ~64% consumption then reaction rate decreases upto 30h with a maximum glycerol conversion of 77.1%. Additionally, we believe that the decomposition of H<sub>2</sub>O<sub>2</sub> is also occurring continuously over our catalyst. Blank experiment was carried out using H<sub>2</sub>O<sub>2</sub> over our catalyst (Cu/SiO<sub>2</sub>-MnO<sub>2</sub>) at reaction temperature and we found that H<sub>2</sub>O<sub>2</sub> is continuously decomposing over the catalyst making the peroxide concentration lower with time. So the oxidation of acrolein to acrylic acid become slow with time (after 50 h).

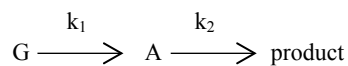
## Kinetic study

Glycerol to acrylic acid occurs in two consecutive steps. 1<sup>st</sup> step is the dehydration step of glycerol, where the glycerol molecule gets converted in to acrolein via intermediate 3-hydroxy propionic acid by the acid sites of the catalyst. While in 2<sup>nd</sup> step is the oxidation of acrolein with H<sub>2</sub>O<sub>2</sub> for the formation of acrylic acid.

Theg steps can be represented as



As the peroxide is used in excess so the equation (2) can be simplified as; two consecutive occurrence of two irreversible pseudo-first order reaction.



Where, k<sub>1</sub> and k<sub>2</sub> is the rate constant of the first and second steps of the reaction, respectively. The rate constant of the first step (k<sub>1</sub>) can be expressed by conventional equation for 1<sup>st</sup> order reaction.

$$C_G/C_{G0} = e^{-k_1 t} \quad (3)$$

Where, C<sub>G</sub> and C<sub>G0</sub> is the final and initial molar concentration of the glycerol at time zero and t respectively.

The rate constant of the second step (k<sub>2</sub>) can be expressed in the form of concentration of acrolein (C<sub>A</sub>) and acrylic acid (C<sub>P</sub>) respectively.

$$d(C_P/C_{G0})/dt = k_2 (C_A/C_{G0}) \quad (4)$$

Initially, when the formation of product is too low then the equation (4) can be rewritten as

$$C_P/C_{G0}t = K_2 (C_A/C_{G0})$$

Now the value of  $k_2$  can be determined from the slope of the linear plot of  $(C_p/C_{G0}t)$  versus  $(C_A/C_{G0})$  and shown in Figure S9. The plot of  $(C_p/C_{G0}t)$  versus  $(C_A/C_{G0})$  made at  $90^\circ\text{C}$  shows the value of  $k_2 = 0.3575 \text{ S}^{-1}$  and exactly fit; thereby it supports our model of pseudo-first order reaction. Based on the model it can be concluded that this is an overall first order reaction. Figure S10.

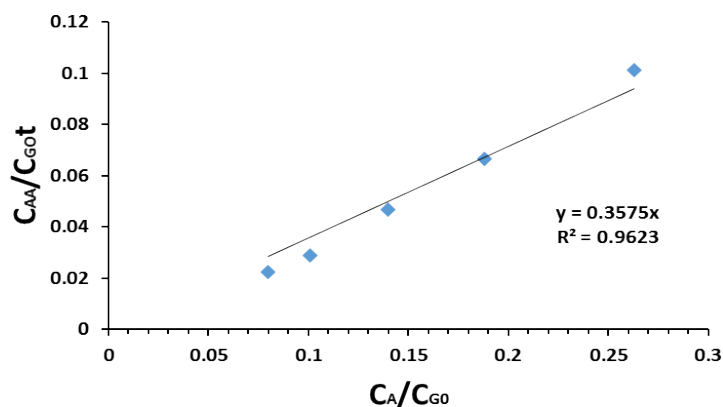


Figure S10. Plot of  $C_{AA}/C_{G0}t$  vs  $C_A/C_{G0}$

Thus the plot of  $(C_p/C_{G0}t)$  versus  $(C_A/C_{G0})$  made at  $90^\circ\text{C}$  shows the value of  $K_2 = 0.3575 \text{ S}^{-1}$  is exactly fit; thereby it supports our mode (Figure S10). Based on the model it can be concluded that this is an overall second order reaction. The rate constant ( $k_2$ ) was calculated in different temperature and Arrhenius plot was used to calculate the activation energy ( $E_a$ ) for the reaction. From, the plot of  $\ln k_2$  versus  $1/T$  (in  $^\circ\text{C}$ ) (Figure S11), activation energy was calculated and found 1.14 KJ/mol.

Figure S11

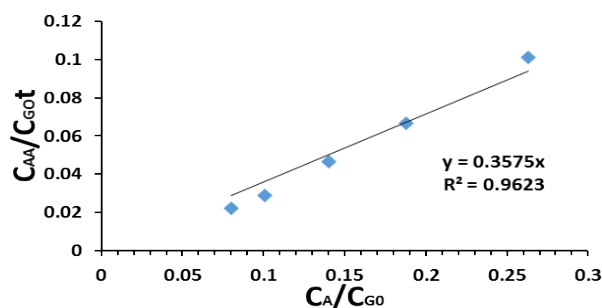


Figure S11. Kinetic Modeling: plot of  $C_{AA}/C_{G0}t$  vs  $C_A/C_{G0}$